*Iranian Journal of Organic Chemistry Vol. 9, No. 4 (2017) 2239-2247*

# A theoretical study of structural and spectral properties on [$^{18}$F]FDG radiopharmaceutical

Mehdi Nabati[a,*] and Ahmad Maghsoudloo-Mahalli[b]

[a]*Chemistry Department, Faculty of Science, Azarbaijan Shahid Madani University, Tabriz, Iran*
[b]*Medical Radiation Department, Faculty of Nuclear Engineering, Central Tehran Branch, Islamic Azad University, Tehran, Iran*

Received: September 2017; Revised: September 2017; October: 2017

**Abstract:** Fluorodeoxyglucose (more precisely 2-deoxy-2-fluoro-D-glucose or [$^{18}$F]FDG for short) is a glucose analogue and is taken up by body cells that are high users of glucose such as brain and cancer cells. This nuclear medicine is a positron emitter radiopharmaceutical that is used for diagnostic applications by positron emission tomography (PET) scan. The present research work studies theoretically the structural and spectral properties, reactivity and stability of this radiopharmaceutical by quantum-mechanical (QM) computations. We use density functional theory (DFT) method for our computations. The molecular electrostatic potential (MEP), frontier molecular orbital (FMO) analysis and natural bond orbital (NBO) population analysis are used for discussion about reactivity and stability subjects of this nuclear medicine. Our computations showed this molecule is a stable structure and has not an ideal chair-form structure. We hope our deductions will give novel ideas about [$^{18}$F]FDG medicine to other researchers.

**Keywords:** DFT study, [$^{18}$F]FDG, Nuclear medicine, Radiopharmaceutical, Reactivity, Stability.

## Introduction

Radiopharmaceuticals or medicinal radio-compounds are a group of pharmaceutical drugs which have radioactivity. Radiopharmaceuticals can be used as diagnostic and therapeutic agents [1]. Radio-pharmacology is the branch of pharmacology that specializes in these agents. The main group of these compounds is the radiotracers used to diagnose dysfunction in body tissues. While not all medical isotopes are radioactive, radiopharmaceuticals are the oldest and still most common such drugs [2]. Nuclear medicine, in a sense, is "radiology done inside out" because it records radiation emitting from within the body rather than radiation that is generated by external sources like X-rays [3].

*Corresponding author. Tel: +98 (413) 4327501; Fax: +98 (413) 4327501, E-mail: mnabati@ymail.com

In addition, nuclear medicine scans differ from radiology as the emphasis is not on imaging anatomy but the function and for such reason; it is called a physiological imaging modality. Single Photon Emission Computed Tomography or SPECT and Positron Emission Tomography or PET scans are the two most common imaging modalities in nuclear medicine [4]. Positron emission tomography (PET) is a nuclear medicine functional imaging technique that is used to observe metabolic processes in the body. The system detects pairs of gamma rays emitted indirectly by a positron-emitting radionuclide (tracer), which is introduced into the body on a biologically active molecule [5]. Three-dimensional images of tracer concentration within the body are then constructed by computer analysis. In modern PET-CT scanners, three dimensional imaging is often accomplished with the aid of a CT X-ray scan performed on the patient during the same session, in the same machine [6].

Fluorine-18 is a positron emitter radionuclide with a half-life of 109.77 minutes. It is used in PET scans. Its decay mode is $_9F^{18} \rightarrow {}_8O^{18} + {}_{+1}e^0$ (1.656 MeV). The positron travels only a few millimetres in the human body before it meets an electron, when both are annihilated producing two gamma ray photons. The energy of each gamma ray photon is 511 MeV, the rest mass of the electron, so presumably the positron loses some energy prior to annihilation. The typical exposure from a PET scan is about 7 mSv. The fluorine-18 production is done by irradiation of the stable oxygen-18 isotope with high energy protons (18 MeV) from a cyclotron. The fluorine-18 production formula is: $_8O^{18} + {}_{+1}p^1 \rightarrow {}_9F^{18} + {}_0n^1$. The target is either normal or enriched water [7]. The half-life of fluorine-18 radionuclide is 109.77 minutes, which means that the radioisotope must be transported post haste. Ideally a nuclear medicine facility at a hospital would have its own cyclotron [8]. Fluorine-18 is used as a radioactive tracer in PET scans mostly as fluorodeoxyglucose (more precisely 2-deoxy-2-fluoro-D-glucose or FDG for short), which is a glucose analogue and is taken up by body cells that are high users of glucose such as brain and cancer cells. The presence of fluorine in the molecule inhibits the body metabolizing it as a normal glucose molecule. Once, the fluorine-18 has decayed to oxygen-18 the normal metabolic process proceeds. A typical dose is 5-10 millicuries or 200-400 MBq administered by saline drip. The patient is scanned an hour later during which the patient should avoid activity so that the FDG does not go to active muscles [9-11].

Computational chemistry is a branch of chemistry that uses computer simulation to assist in solving chemical problems. It uses methods of theoretical chemistry, incorporated into efficient computer programs, to calculate the structures and properties of molecules and solids [12]. Theoretical chemistry unites principles and concepts common to all branches of chemistry [13]. Within the framework of theoretical chemistry, there is a systematization of chemical laws, principles and rules, their refinement and detailing, the construction of a hierarchy. The central place in theoretical chemistry is occupied by the doctrine of the interconnection of the structure and properties of molecular systems. It uses mathematical and physical methods to explain the structures and dynamics of chemical systems and to correlate, understand, and predict their thermodynamic and kinetic properties [14]. In the most general sense, it is explanation of chemical phenomena by methods of theoretical physics. In contrast to theoretical physics, in connection with the high complexity of chemical systems, theoretical chemistry, in addition to approximate mathematical methods, often uses semi-empirical and empirical methods.

In recent years, it has consisted primarily of quantum chemistry, such as the application of quantum mechanics to problems in chemistry. Other major components include molecular dynamics, statistical thermodynamics and theories of electrolyte solutions, reaction networks, polymerization, catalysis, molecular magnetism and spectroscopy [15]. Modern theoretical chemistry may be roughly divided into the study of chemical structure and the study of chemical dynamics. The former includes studies of: electronic structure, potential energy surfaces, and force fields; vibrational-rotational motion; equilibrium properties of condensed-phase systems and macro-molecules [16].

In the present research work, we do the theoretical studies on the [$^{18}$F]FDG nuclear medicine by density functional theory (DFT) computational method. In this way, we investigate and discuss the structural, stability, reactivity, and spectral properties and natural bond orbital (NBO) population analysis of the mentioned radiopharmaceutical. We hope that our findings can solve the complicated subjects for this radiopharmaceutical.

## Results and discussion

In this research, the [$^{18}$F]FDG nuclear medicine was studied. The structure of the molecule is shown in Scheme **1**.

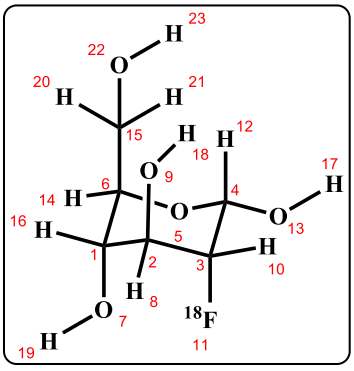


**Scheme 1:** The molecular structure of [$^{18}$F]FDG with atomic numbering.

The structure of this radiopharmaceutical was optimized by density functional theory (DFT) method at B3LYP/6-31+G(d,p) level of theory. The optimized structure is shown in Figure **1**. Here, the structural and spectral properties of this medicine will be discussed.

Also, we study the reactivity and stability of [$^{18}$F]FDG molecular structure.

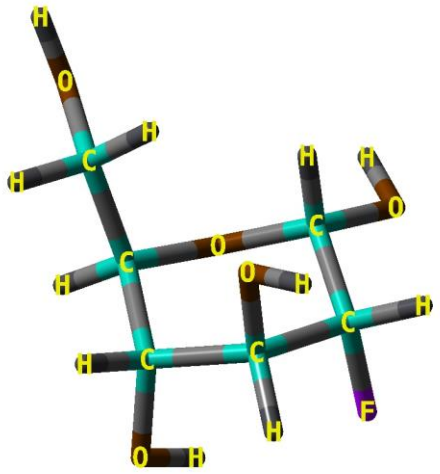

**Figure 1:** The optimized structure of [$^{18}$F]FDG.

*Structural properties of [$^{18}$F]FDG:*

After optimization of structure of the studied nuclear medicine, the bond lengths, bond angles and dihedral angles of the molecular structure were collected and listed in Table **1**. The investigation on the geometrical structure of the studied radiopharmaceutical can give us good information about stability and reactivity of the compound. From the data of the Table **1**, we can see the bond length of C-C and C-H bonds vary in range 1.53-1.55 and 1.00-1.10 Angstrom, respectively. Also, it can be seen from the data that the bond lengths of the O-H and C-$^{18}$F bonds are 0.97 and 1.41 Angstrom, respectively. In comparison C6-O5 bond (1.44 Å) with C4-O5 bond (1.42 Å), the C4-O5 bond is smaller because of the connecting of the C4 atom to two oxygen atoms. The data of the bond angles indicates that all bond angles into the sextet ring are more than 104.5 degree. It happens because of electronegative substituents on carbon atoms of the ring. The C4-O5-C6 angle is more among all bond angles into the ring. The reason of this bond angle is the nonbonding electron pairs of the oxygen-5 atom. In contrast, the smaller bond angle into the ring is related to the O5-C6-C1 bond angle because of the large substituent on carbon-6 atom. Also, the fluorine atom causes the low amount of bond angles containing this more electronegative atom. On the other hand, it can be deduced from the dihedral angle data that our studied structure does not show the ideal chair-form structure, and the real structure for this compound is twisted-chair.

**Table 1:** Bond lengths, bond angles and dihedral angles data of the studied molecule.

| Bonds | Bond length (Angstrom) | Bond angle | Angle (degree) |
|---|---|---|---|
| C1-C2 | 1.546 | C1-C2-C3 | 111.583 |
| C2-C3 | 1.540 | C2-C3-C4 | 110.620 |
| C3-C4 | 1.528 | C3-C4-O5 | 110.814 |
| C4-O5 | 1.418 | C4-O5-C6 | 115.066 |
| C6-O5 | 1.438 | O5-C6-C1 | 109.601 |
| C1-C6 | 1.543 | C6-C1-C2 | 112.616 |
| C1-O7 | 1.422 | C2-C3-F11 | 107.686 |
| O7-H19 | 0.969 | C4-C3-F11 | 109.478 |
| C1-H16 | 1.094 | H10-C3-F11 | 107.088 |
| C2-H8 | 1.096 | H16-C1-O7-H19 | 178.999 |
| C2-O9 | 1.433 | H14-C6-C1-H16 | 77.775 |
| O9-H18 | 0.966 | C15-C6-C1-O7 | 157.453 |
| C3-F11 | 1.406 | H8-C2-C1-O7 | 42.307 |
| C3-H10 | 1.096 | H8-C2-O9-H18 | 40.681 |
| C4-O13 | 1.394 | H8-C2-C3-F11 | 47.369 |
| O13-H17 | 0.968 | O9-C2-C3-F11 | 169.228 |
| C4-H12 | 1.102 | H12-C4-C3-F11 | 176.237 |
| C6-H14 | 1.094 | O13-C4-C3-F11 | 55.451 |
| C6-C15 | 1.531 | O5-C4-C3-F11 | 63.584 |
| C15-H20 | 1.100 | C1-C2-C3-F11 | 71.173 |
| C15-H21 | 1.095 | H12-C4-C3-H10 | 58.604 |
| C15-O22 | 1.427 | O13-C4-C3-H10 | 62.182 |
| O22-H23 | 0.965 | O22-C15-C6-O5 | 57.686 |

Table **2** shows the bond orders (B.O.) data of the molecular structure. The Wiberg bond orders were achieved by NBORead computation method in Gaussian software. From the data of the Table **2**, the bond orders of C-C, C-O and C-H bonds are in 0.97-0.98, 0.89-0.90 and 0.88-0.90 ranges, respectively. In the case of C-O bonds, we can see that the cyclic C-O bonds are weaker than the acyclic C-O bonds. Also, it can be seen from the data that the weakness order of O-H bonds is: O7-H19 (0.708) > O13-H17 (0.714) > O9-H18 (0.724) > O22-H23 (0.737). So, the hydrogen-19 is the weakest hydrogen atom among all O-H hydrogen atoms, and its acidity property is more.
Analysis of electronic composition of bonds in a molecular structure is done by natural bond orbital (NBO) computations [17].

**Table 2:** Bond orders (B.O.) data of the studied molecule.

| Bonds | Bond order (B.O.) |
|---|---|
| C1-C2 | 0.970 |
| C2-C3 | 0.974 |
| C3-C4 | 0.972 |
| C4-O5 | 0.901 |
| C6-O5 | 0.892 |
| C1-C6 | 0.980 |
| C1-O7 | 0.949 |
| O7-H19 | 0.708 |
| C1-H16 | 0.887 |
| C2-H8 | 0.896 |
| C2-O9 | 0.921 |
| O9-H18 | 0.724 |
| C3-F11 | 0.825 |
| C3-H10 | 0.901 |
| C4-O13 | 0.972 |
| O13-H17 | 0.714 |
| C4-H12 | 0.887 |
| C6-H14 | 0.880 |
| C6-C15 | 0.992 |
| C15-H20 | 0.909 |
| C15-H21 | 0.908 |
| C15-O22 | 0.937 |
| O22-H23 | 0.737 |

Table **3** collects the data of the NBO population analysis of [$^{18}$F]FDG nuclear medicine structure. The data of the Table **3** indicates that the C4 atom uses more p orbital in composition of the C4-O5 bond than the C4-O13 bond. It proves that the cyclic C-O bond bears more strain pressure than the acyclic C-O bond. Corresponding to the carbon-4 atom, the oxygen-5 atom uses more p orbitals than the oxygen-13 atom. For this reason, the hybrid of the C4-H12 bond is constructs from lower p orbitals of carbon-4 atom. So, this causes the acidic property of hydrogen-12 atom. In other hand, the carbon-3 and fluorine-11 atoms use more p and s orbitals in construction of C3-F11 bond, respectively. It happens because of the more electronegativity of fluorine atom.

*Reactivity prediction of [$^{18}$F]FDG:*

In chemistry, frontier molecular orbitals (FMOs) theory is an application of molecular orbital (MO) theory describing HOMO/LUMO interactions. Fukui realized that a good approximation for reactivity could be found by looking at the frontier molecular orbitals (HOMO and LUMO) [18-20]. Figure **2** indicates the frontier molecular orbitals graph of [$^{18}$F]FDG nuclear medicine. Our computations show the energies -7.34 and -0.58 eV for HOMO and LUMO, respectively. The high content of HOMO/LUMO energies gap (6.76 eV) shows the high stability and low reactivity of the studied molecule.

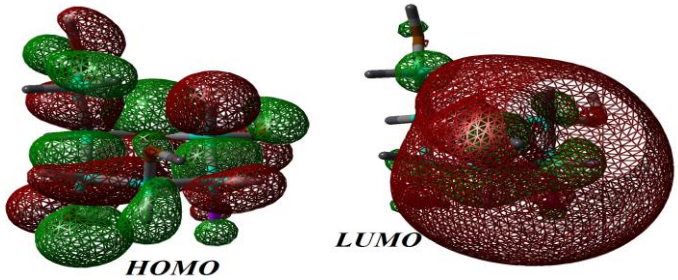


**Figure 2:** The frontier molecular orbitals of [$^{18}$F]FDG.

The density of states (DOS) graph of molecular structure is shown in Figure **3**. The DOS of a system describes the number of states per interval of energy at energy level available to be occupied [21]. We can see from the Figure **3** that the virtual orbitals have more states than occupied orbitals. Also, the both of frontier molecular orbitals (H/L) show lower number of states than all molecular orbitals. So, the transition of electron from HOMO to LUMO happens hardly. For this, the studied molecule is a more stable compound.

**Table 3:** Natural bond orbitals (NBOs) analysis data of the studied molecule.

| Bonds | Occupancy | Population/Bond orbital/Hybrids |
|---|---|---|
| σ(C1-C2) | 1.97716 | 49.08% C1 ($sp^{2.81}$), 50.92% C2 ($sp^{2.69}$) |
| σ(C2-C3) | 1.98084 | 49.93% C2 ($sp^{2.80}$), 50.07% C3 ($sp^{2.60}$) |
| σ(C3-C4) | 1.98142 | 50.53% C3 ($sp^{2.63}$), 49.47% C4 ($sp^{2.53}$) |
| σ(C4-O5) | 1.98959 | 32.69% C4 ($sp^{3.69}d^{0.01}$), 67.31% O5 ($sp^{2.67}$) |

| | | |
|---|---|---|
| σ(C6-O5) | 1.98393 | 32.24% C6 ($sp^{4.21}d^{0.01}$), 67.76% O5 ($sp^{2.49}$) |
| σ(C1-C6) | 1.98158 | 50.04% C1 ($sp^{2.66}$), 49.96% C6 ($sp^{2.64}$) |
| σ(C1-O7) | 1.99082 | 34.25% C1 ($sp^{3.73}d^{0.01}$), 65.75% O7 ($sp^{2.36}$) |
| σ(O7-H19) | 1.98878 | 76.36% O7 ($sp^{3.38}$), 23.64% H19 (s) |
| σ(C1-H16) | 1.97159 | 62.91% C1 ($sp^{2.96}$), 37.09% H16 (s) |
| σ(C2-H8) | 1.98270 | 62.86% C2 ($sp^{2.82}$), 37.14% H8 (s) |
| σ(C2-O9) | 1.98975 | 33.44% C2 ($sp^{3.87}d^{0.01}$), 66.56% O9 ($sp^{2.34}$) |
| σ(O9-H18) | 1.98974 | 75.86% O9 ($sp^{3.54}$), 24.14% H18 (s) |
| σ(C3-F11) | 1.99260 | 27.30% C3 ($sp^{4.55}d^{0.01}$), 72.70% F11 ($sp^{2.71}$) |
| σ(C3-H10) | 1.97974 | 62.01% C3 ($sp^{2.73}$), 37.99% H10 (s) |
| σ(C4-O13) | 1.99337 | 33.97% C4 ($sp^{3.31}d^{0.01}$), 66.03% O13 ($sp^{2.23}$) |
| σ(O13-H17) | 1.98557 | 76.11% O13 ($sp^{3.64}$), 23.89% H17 (s) |
| σ(C4-H12) | 1.97933 | 61.34% C4 ($sp^{2.66}$), 38.66% H12 (s) |
| σ(C6-H14) | 1.97122 | 63.84% C6 ($sp^{3.01}$), 36.16% H14 (s) |
| σ(C6-C15) | 1.98329 | 50.58% C6 ($sp^{2.52}$), 49.42% C15 ($sp^{2.64}$) |
| σ(C15-H20) | 1.98065 | 61.19% C15 ($sp^{3.01}$), 38.81% H20 (s) |
| σ(C15-H21) | 1.98661 | 61.74% C15 ($sp^{2.80}$), 38.26% H21 (s) |
| σ(C15-O22) | 1.99528 | 33.61% C15 ($sp^{3.66}d^{0.01}$), 66.39% O22 ($sp^{2.41}$) |
| σ(O22-H23) | 1.98954 | 75.32% O22 ($sp^{3.69}$), 24.68% H23 (s) |
| $LP_1$(F11) | 1.99149 | F11 ($sp^{0.37}$) |
| $LP_2$(F11) | 1.96986 | F11 ($sp^{99.99}d^{2.72}$) |
| $LP_3$(F11) | 1.96744 | F11 ($sp^{99.99}d^{0.18}$) |
| $LP_1$(O10) | 1.95871 | O10 ($sp^{1.27}$) |
| $LP_2$(O10) | 1.92027 | O10 ($sp^{99.99}d^{1.53}$) |

The molecular electrostatic potential (MEP) is a good guide in assessing the molecules reactivity towards positively or negatively charged reactants. The MEP is typically visualized through mapping its values onto the surface reflecting the molecules boundaries [22, 23]. Figure **4** indicates the MEP graph of [$^{18}$F]FDG radiopharmaceutical. In graph, the blue and red colors show the positive and negative potentials. As can be seen from the Figure **4**, whole molecular structure has uniform on its surface (green color). It shows that all atoms of structure have same charge on their surface. So, this proves the high stability of our studied molecule. In other hand, the MEP graph of frontier orbitals is shown in Figure **5**. The HOMO and LUMO indicate low negative and positive charge on the surface of their atoms, respectively.

So, the transition of electron can be happened from HOMO to LUMO with high content of energy (>6.76 eV). This hard electronic transition between frontier orbitals show the more stability and low stability of [$^{18}$F]FDG nuclear medicine.

*UV-Vis, IR and NMR spectra prediction of [$^{18}$F]FDG*

In chemistry, the identification of chemical molecules is done by spectroscopy methods [24]. Here, the UV-Vis, IR and NMR spectral properties of the [$^{18}$F]FDG nuclear medicine are investigated and discussed.

The UV-Vis spectrum of the studied molecule is indicated in Figure **6**. In the UV-Vis spectrum, the peak at wavelength 205.097 nm with energy 48757.359 cm$^{-1}$ is related to the HOMO to LUMO transition. The other transitions (HOMO to LUMO+1 (85%), HOMO-2 to LUMO+1 (8%) and HOMO to LUMO+2 (3%)) take place at wavelength 198.994 nm with energy 50252.721 cm$^{-1}$. Also, the HOMO-1 to LUMO transition is shown at wavelength 194.603 nm with energy 51386.744 cm$^{-1}$.

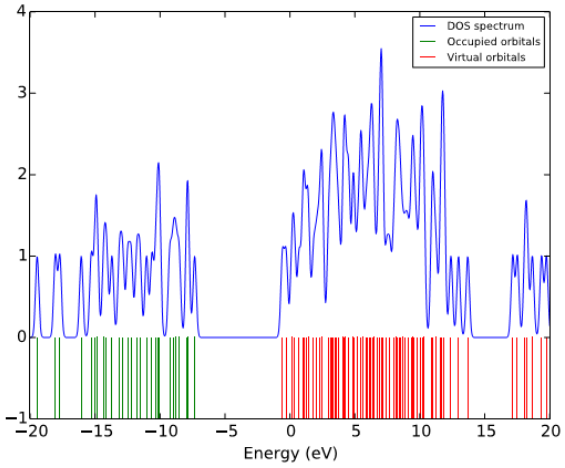


**Figure 3:** The density of states (DOS) graph of [$^{18}$F]FDG.

Figure **7** indicates the IR spectrum of the studied molecule. IR [Harmonic frequencies (cm$^{-1}$), intensities (KM/Mole)]: 63.8020 (4.9876), 87.6652 (1.0059), 137.7466 (7.1538), 179.2777 (4.8339), 190.6981 (4.2693), 205.7075 (17.2687), 222.6924 (89.1703), 239.5978 (6.2382), 251.6257 (37.5833), 264.0643 (134.1325), 285.5752 (70.4193), 324.3715 (14.0579),

346.5343 (14.4790), 408.8280 (103.2097), 414.6304 (11.4287), 428.1914 (4.4408), 475.7993 (24.4026), 529.6136 (9.0133), 575.9037 (4.9860), 591.7550 (28.3962), 718.5881 (22.4680), 806.9587 (55.3200), 851.8437 (20.0129), 889.0700 (5.3569), 901.1640 (42.5006), 985.8928 (6.6528), 1038.0017 (77.3088), 1048.5032 (52.8407), 1059.6434 (168.2542), 1077.2050 (18.6034), 1079.9984 (74.0916), 1092.1705 (88.6539), 1109.5967 (65.1843), 1124.5229 (73.1720), 1173.7182 (92.0587), 1209.5026 (35.8774), 1212.8760 (7.0033), 1237.6500 (18.7335), 1256.2335 (54.8605), 1280.6113 (17.8227), 1294.2974 (42.5881), 1322.7003 (11.9943), 1330.2623 (0.5265), 1349.8292 (1.2028), 1384.5629 (6.9072), 1396.3220 (32.3112), 1399.9111 (7.8806), 1419.0850 (3.7059), 1435.3735 (46.5041), 1453.1481 (1.1535), 1464.7830 (12.1522), 1526.6313 (8.1258), 2996.7895 (31.0976), 3008.0712 (45.2031), 3063.5989 (24.5447), 3078.4697 (0.4400), 3079.8954 (43.4523), 3092.2444 (19.3665), 3103.8163 (26.8511), 3786.2209 (55.3523), 3810.1757 (52.5537), 3833.0744 (42.6183) and 3839.3833 (36.4289).

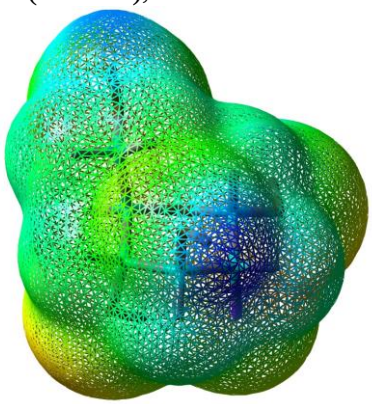

**Figure 4:**The molecular electrostatic potential (MEP) graph of [$^{18}$F]FDG.

The NMR technique is a good method for identification of the structure of the organic compounds [25]. The $^{1}$H and $^{13}$C chemical shifts of the [$^{18}$F]FDG nuclear medicine are listed in Table **4**. The theoretical chemical shifts data is compared to the experimental values. The Figure **8** indicates the comparison between the theoretical and experimental $^{1}$H and $^{13}$C chemical shifts of the molecular structure at studied computational method. The large correlation coefficient (R=0.995) shows the accuracy of our computations. From the data of Table **4**, the H12 nucleus is more de-shielded nucleus among all hydrogen atoms of [$^{18}$F]FDG structure, because the carbon atom of C-H12 bond is connected to two oxygen atoms. On other hand, the C3 nucleus is the de-shielded carbon atom, because it is connected to fluorine atom. Also, we can see that the hydrogen atoms of the O-H bonds show big difference between theoretical and experimental chemical shifts. This difference happens because of the proton exchange by O-H functional groups.

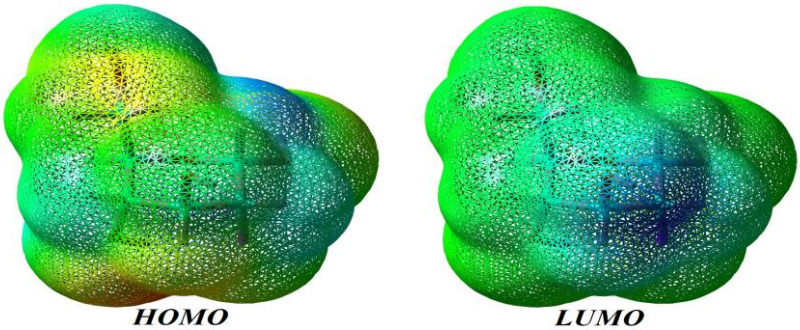


**Figure 5:** The MEP graphs of HOMO/LUMO orbitals of the studied molecule.

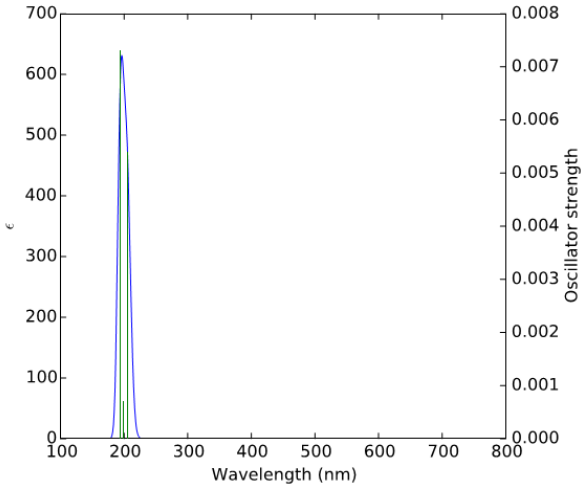


**Figure 6:** The UV-Vis spectrum of the studied molecule.

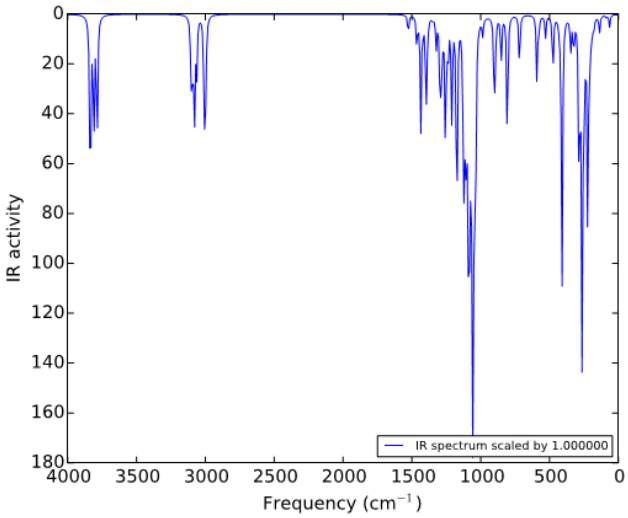


**Figure 7:** The IR spectrum of the studied molecule.

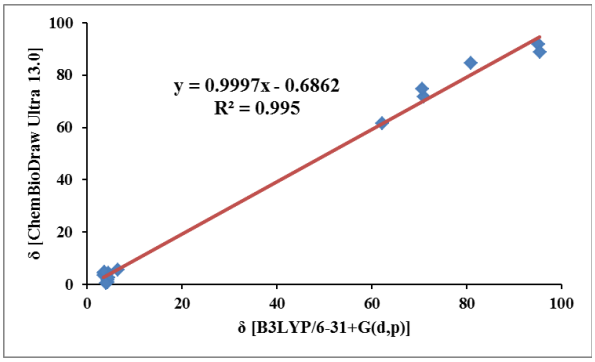


**Figure 8:** The relationship between theoretical and experimental NMR chemical shifts of the studied structure.

**Table 4:** The $^{1}H$ and $^{13}C$ chemical shifts of the studied molecule.

| Nucleus | Chemical Shift (ppm) | |
|---|---|---|
| | Theoretical chemical shifts ($\delta = \delta_{TMS} - \delta'$) | δ (Chemical shifts from ChemBioDraw Ultra 13.0) |
| H-8 | 4.233 | 4.400 |
| H-10 | 4.400 | 3.430 |
| H-12 | 5.546 | 6.400 |
| H-14 | 4.573 | 3.600 |
| H-16 | 3.358 | 3.600 |
| H-17 | 1.637 | 4.320 |
| H-18 | 0.837 | 4.370 |
| H-19 | 2.632 | 4.510 |
| H-20 | 3.418 | 3.510 |
| H-21 | 4.625 | 3.570 |
| H-23 | 0.375 | 3.940 |
| C-1 | 71.744 | 70.900 |
| C-2 | 74.586 | 70.600 |
| C-3 | 91.832 | 95.100 |
| C-4 | 88.837 | 95.300 |
| C-6 | 84.675 | 80.900 |
| C-15 | 61.539 | 62.200 |

## Computational method

In present research work, all computations were performed by Gaussian 03 package [26] using density functional theory (DFT) computational method by B3LYP functional with 6-31+G(d,p) basis set. The computations were done in the gas phase at room temperature. There was no imaginary frequency in IR computation for molecular structure. It proves accuracy of our computations.

## Conclusions

In the present work, structural properties of structural and spectral properties, reactivity and stability of [$^{18}$F]FDG as a nuclear medicine have been investigated theoretically by using quantum chemical treatment. Full geometrical optimization of the structure was performed using density functional theory (DFT, B3LYP) at the level of 6-31+G(d,p) basis set. According to the results, we can be concluded as follows:

a. The studied structure does not show the ideal chair-form structure, and the real structure for this compound is twisted-chair.

b. The hydrogen-19 is the weakest hydrogen atom among all O-H hydrogen atoms, and its acidity property is more.

c. The carbon-3 and fluorine-11 atoms use more p and s orbitals in construction of C3-F11 bond, respectively.

d. The high content of HOMO/LUMO energies gap (6.76 eV) shows the high stability and low reactivity of the studied molecule.

e. In the molecular structure, the virtual orbitals have more states than occupied orbitals.

f. The MEP graph shows that all atoms of structure have same charge on their surface. So, this proves the high stability of our studied molecule.

g. The HOMO and LUMO indicate low negative and positive charge on the surface of their atoms, respectively. So, the transition of electron can be happened from HOMO to LUMO with high content of energy (>6.76 eV). This hard electronic transition between frontier orbitals show the more stability and low stability of [$^{18}$F]FDG nuclear medicine.

h. The UV-Vis, IR and NMR spectra gave us more information about structural properties of the [$^{18}$F]FDG nuclear medicine.

## Acknowledgments

The corresponding author is grateful to Doctor Hojjatollah Salehi and Mr. Hossein Abbasi for providing valuable suggestions.

## References

[1] Fallahi, B.; Esmaeili, A.; Beiki, D.; Oveisgharan, S.; Noorollahi-Moghaddam, H.; Erfani, M.; Tafakhori, A.; Rohani, M.; Fard-Esfahani, A.; Emami-Ardekani, A.; Geramifar, P.; Eftekhari, M. *Ann. Nucl. Med.*, **2016**, *30*, 153-162.

[2] Erfani, M.; TShafiei, M. *Nucl. Med. Biol.,* **2014**, *30,* 317-321.
[3] Erfani, M.; TShafiei, M.; Charkhlooie, G.; Goudarzi, M. *Iran J. Nucl. Med.*, **2015**, *23,* 15-20.
[4] Fischer, S.; Hiller, A.; Smits, R.; Hoepping, A.; Funke, U.; Wenzel, B.; Cumming, P.; Sabri, O.; Steinbach, J.; Brust, P. *Appl. Radiat. Isot.*, **2013**, *74*, 128-136.
[5] Sabri, O.; Becker, G.; Meyer, P. M.; Hesse, S.; Wilke, S.; Graef, S.; Patt, M.; Luthardt, J.; Wagenknecht, G.; Hoepping, A. *J. Neurolmage*, **2015**, *118*, 199-208.
[6] Smits, R.; Fischer, S.; Hiller, A.; Deuther-Conrad, W.; Wenzel, B.; Patt, M.; Cumming, P.; Steinbach, J.; Sabri, O.; Brust, P.; Hoepping, A. *Bioorg. Med. Chem.*, **2014**, *22,* 804-812.
[7] Shankar, L. K.; Hoffman, J. M.; Bacharach, S.; Graham, M. M.; Karp, J.; Lammertsma, A. A.; Larson, S.; Mankoff, D. A.; Siegel, B. A.; Abbeele, A. V.; Yap, J.; Sullivan, D. *J. Nucl. Med.,* **2006**, *47,* 1059-1066.
[8] McConnell, D.; Jordan, L.; Kemp, B.; Lowe, W. *J. Nucl. Med.,* **2016**, *57,* 2640-2648.
[9] Sheikhbahaei, S.; Marcus, C.; Wray, R.; Rahmim, A.; Lodge, M. A.; Subramaniam, R. M. *Nucl. Med. Commun.,* **2016**, *37,* 288-296.
[10] Jones, T. A.; Reddy, N.; Wayte, S.; Adesanye, O.; Barber, T.; Hutchinson, C. *Clin. Radiol.,* **2016**, *71,* S8-S9.
[11] Vadrucci, M.; Serio, G.; Baroli, A. *Endocrinol. Metab.,* **2016**, *31,* 343-344.
[12] Nabati, M.; Mahkam, M. *Inorg. Chem. Res.,* **2016**, *1,* 131-140.
[13] Nabati, M. *J. Phys. Theor. Chem. IAU Iran,* **2015**, *12,* 325-338.
[14] Nabati, M.; Mahkam, M.; Atani, Y. G. *J. Phys. Theor. Chem. IAU Iran,* **2016**, *13,* 35-59.
[15] Nabati, M.; Mahkam, M. *Org. Chem. Res.,* **2016**, *2,* 70-80.
[16] Nabati, M. *Iran. J. Org. Chem.,* **2016**, *8,* 1703-1716.
[17] Nabati, M. *J. Phys. Theor. Chem. IAU Iran,* **2016**, *13,* 133-146.
[18] Nabati, M.; Mahkam, M. *J. Phys. Theor. Chem. IAU Iran,* **2015**, *12,* 33-43.
[19] Nabati, M.; Mahkam, M. *Silicon,* **2016**, *8,* 461-465.
[20] Nabati, M.; Mahkam, M. *J. Phys. Theor. Chem. IAU Iran,* **2015**, *12,* 121-136.
[21] Nabati, M.; Mahkam, M. *Iran. J. Org. Chem.,* **2015**, *7,* 1463-1472.
[22] Nabati, M.; Mofrad, M. H.; Kermanian, M.; Sarshar, S. *Iran. J. Org. Chem.,* **2017**, *9,* 1981-1993.
[23] Nabati, M.; Salehi, H. *Iran. J. Org. Chem.,* **2017**, *9,* 2013-2023.
[24] Nabati, M. *Iran. J. Org. Chem.*, **2017**, *9,* 2045-2055.
[25] Nabati, M.; Kermanian, M.; Maghsoudloo-Mahalli, A.; Sarshar, S. *Iran. J. Org. Chem.,* **2017**, *9,* 2067-2077.
[26] Frisch, M. J.; Trucks, G. W.; Schlegel, H. B.; Scuseria, G. E.; Robb, M. A.; Cheeseman, J. R.; Montgomery Jr., J. A.; Vreven, T.; Kudin, K. N.; Burant, J. C.; Millam, J. M.; Iyengar, S. S.; Tomasi, J.; Barone, V.; Mennucci, B.; Cossi, M.; Scalmani, G.; Rega, N.; Petersson, G. A.; Nakatsuji, H.; Hada, M.; Ehara, M.; Toyota, K.; Fukuda, R.; Hasegawa, J.; Ishida, M.; Nakajima, T.; Honda, Y.; Kitao, O.; Nakai, H.; Klene, M.; Li, X.; Knox, J. E.; Hratchian, H. P.; Cross, J. B.; Adamo, C.; Jaramillo, J.; Gomperts, R.; Stratmann, R. E.; Yazyev, O.; Austin, A. J.; Cammi, R.; Pomelli, C.; Ochterski, J. W.; Ayala, P. Y.; Morokuma, K.; Voth, G. A.; Salvador, P.; Dannenberg, J. J.; Zakrzewski, V. G.; Dapprich, S.; Daniels, A. D.; Strain, M. C.; Farkas, O.; Malick, D. K.; Rabuck, A. D.; Raghavachari, K.; Foresman, J. B.; Ortiz, J. V.; Cui, Q.; Baboul, A. G.; Clifford, S.; Cioslowski, J.; Stefanov, B. B.; Liu, G.; Liashenko, A; Piskorz, P.; Komaromi, I.; Martin, R. L.; Fox, D. J.; Keith, T.; Al-Laham, M. A.; Peng, C. Y.; Nanayakkara, A.; Challacombe, M.; Gill, P. M. W.; Johnson, B.; Chen, W.; Wong, M. W.; Gonzalez, C.; Pople, J. A. *Gaussian 03. Revision B.01*. Gaussian Inc. Wallingford. CT. **2004**.